AD-A083 953 LESCHACK ASSOCIATES LTD SILVER SPRING MD F/G 8/7
RAPID RECONNAISSANCE OF GEOTHERMAL PROSPECTS USING SHALLOW TEMP--ETC(U)
MAR 80 L A LESCHACK, J E LEWIS, D C CHANG N00014-78-C-0535
UNCLASSIFIED TR-3 NL

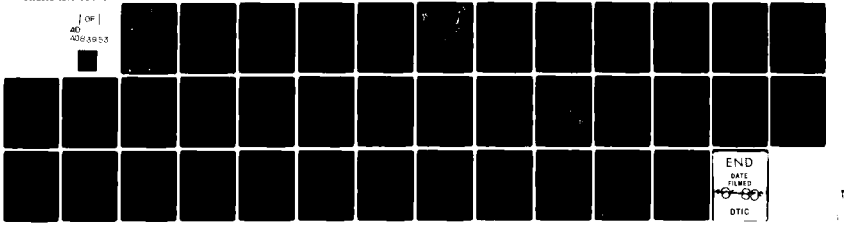

RAPID RECONNAISSANCE OF GEOTHERMAL PROSPECTS USING SHALLOW TEMPERATURE SURVEYS

by

Leonard A. LeSchack, John E. Lewis and David C. Chang

Third Technical Report

LeSchack Associates, Ltd.*

Suite 116
1111 University Blvd. W.
Silver Spring,
Maryland 20902, U.S.A.
(301) 649-1670

P.O. Box 88
San Ramon,
California 94583, U.S.A.
(415) 449-1077

See 1473 in back.

Prepared for the United States
DEPARTMENT OF ENERGY
Under Contract EG-77-C-01-4021
and
OFFICE OF NAVAL RESEARCH
Under Contract N00014-78-C-0535

MARCH 1980

*Formerly Development and Resources Transportation Co.

463:RSA:716:tam
79u460-595

MANDATORY DISTRIBUTION LIST
UNCLASSIFIED TECHNICAL REPORTS, REPRINTS, AND FINAL REPORTS
PUBLISHED BY CONTRACTORS OF THE
EARTH PHYSICS PROGRAM
OFFICE OF NAVAL RESEARCH

(October 1979)

Chief of Naval Research
Department of the Navy
800 North Quincy Street
Arlington, Virginia 22217
Code 100C1 (1)
Code 460 (1)
Code 463 (5)
Code 480 (1)

Commanding Officer
Office of Naval Research
Branch Office (1)
* (ONR Branch Office for contractor area)

Director
Naval Research Laboratory
Code 2627
Washington, D.C. 0375 (6)

Office of Research, Development, Test, and Evaluation
Department of the Navy
Code NOP-987J
Washington, D.C. 20350 (1)

Director
Defense Advanced Research
Projects Agency
1400 Wilson Boulevard
Arlington, Virginia 22209 (1)

Air Force Office of
Scientific Research
Department of the Air Force
Directorate of Physics (MPG)
Building 410
Bolling Air Force Base
Washington, D.C. 20332 (1)

Army Research Office
Department of the Army
Geosciences Division
Box 12211
Research Triangle Park,
North Carolina 27709 (1)

Defense Documentation Center
Building 5
Cameron Station
Alexandria, Virginia 22314 (12)

Administrative Contracting
Office (ACO) (1)
* (Given in Block 6 of Award/Contract Form 26-103)

* Address to be determined by each contractor.

Enclosure 1

ABSTRACT

In this final report, an Annual Wave Correction Model is constructed. The model makes rapid reconnaissance of geothermal prospects using shallow temperature surveys a reality.

The model is tested using data previously obtained at the Coso KGRA. Inputs are surface meteorological data gathered during a 15 month period, soil thermal diffusivity data derived from previous studies in this series, and surface roughness and albedo measured at the site. Computations are made to determine the normal, i.e., non-anomalous temperatures at 2-m depth, for the period 22-24 September 1977, for each of the 102 stations at Coso. The observed 2-m temperatures recorded at these stations during this period and corrected for elevation are compared to the normal temperatures, and a residual anomaly map has been drawn. The map compares favorably to the mean annual temperature map for the same area.

We conclude that a 2-m temperature survey may be conducted at any time and appropriately corrected with the Annual Temperature Correction Model and easily obtained ancillary data. Our model produces a residual map with an accuracy of $\pm$ 1.9°C., adequate for anomalies of the magnitude found at Coso.

We studied the effect of topography on sub-surface isotherms at Coso KGRA using a model (FINITEG) developed by Lee. The model predicted sub-surface temperatures to a depth of 0.75 km in the area of Cactus Peak. The model takes into account 100 m of topographical change and the effects of three anomalous regions near the surface, representing the soil in which the measurements were made. Within the resolution of the model, the isotherms conform to the topography; the contour interval is essentially unvarying as it approaches the surface, even though the isotherms pass through thin soil layers of different thermal conductivity.

We conclude that in geological settings in the Basin and Range Province, where there is some topographic relief and the 2-m temperature measurements are made in a thin soil layer overlying a more conductive bedrock, there are no significant distortions to a 2-m temperature contour map. We can emplace our 2-m survey holes with relatively little concern for topography or modest variations in soil conditions.

CONTENTS

1. Introduction

This is the third and final report on the rapid reconnaissance of geothermal prospects using shallow temperature surveys. The first report, LeSchack *et al* (1977), showed how 2-m temperature measurements made in the summer of 1977 produced the same contour patterns as temperature measurements at 10-m depth at Long Valley, California, and at 30-m depth at Coso Hot Springs KGRA, California (Figure 1). Elevation corrections, i.e., corrections for the adiabatic lapse rate, were the only ones made to our 2-m temperature measurements.

The second report, LeSchack *et al* (1979), discussed the additional temperature measurements made at Long Valley and those made during the winter of 1977 and the spring and summer of 1978 at Coso. We observed the seasonal variations of temperature patterns due to surface effects. Although temperature pattern variations at 2 m due to surface effects at Coso were not significant enough to affect the interpretation of this strong anomaly, they did affect the interpretation of shallow temperature anomalies at sites such as Upsal Hogback, Nevada, where the anomaly is weaker. We found in general that surface effects must be corrected in a shallow temperature survey. We showed that corrections were required for elevation, surface albedo and roughness, and soil thermal diffusivity.

In our previous reports we discussed how we measured these parameters and the effects of groundwater. We concluded that making useful shallow temperature measurements where there is a modest amount of groundwater flow needn't be a hopeless task. Though it often complicates the interpretation of the results, it does not invalidate application of the technique.

In the current report we discuss how all these corrections may be applied to 2-m temperature data taken at any given time. This permits a shallow temperature survey to be conducted at any time of year with temperature and correction measurements being made at the same time. This is the major requirement for a quick, cost-effective reconnaissance temperature survey.

2. The Steps to Conduct a Shallow Temperature Survey*

As stated in LeSchack *et al* (1979), the steps essential to conduct a SHALLO-TEMP^{TM} survey are:

(a) At each site drill two adjacent 2-m holes.

(b) Insert thermistor probe in one, thermal conductivity probe in the other.

*We call this complete survey a SHALLO-TEMP^{TM} survey

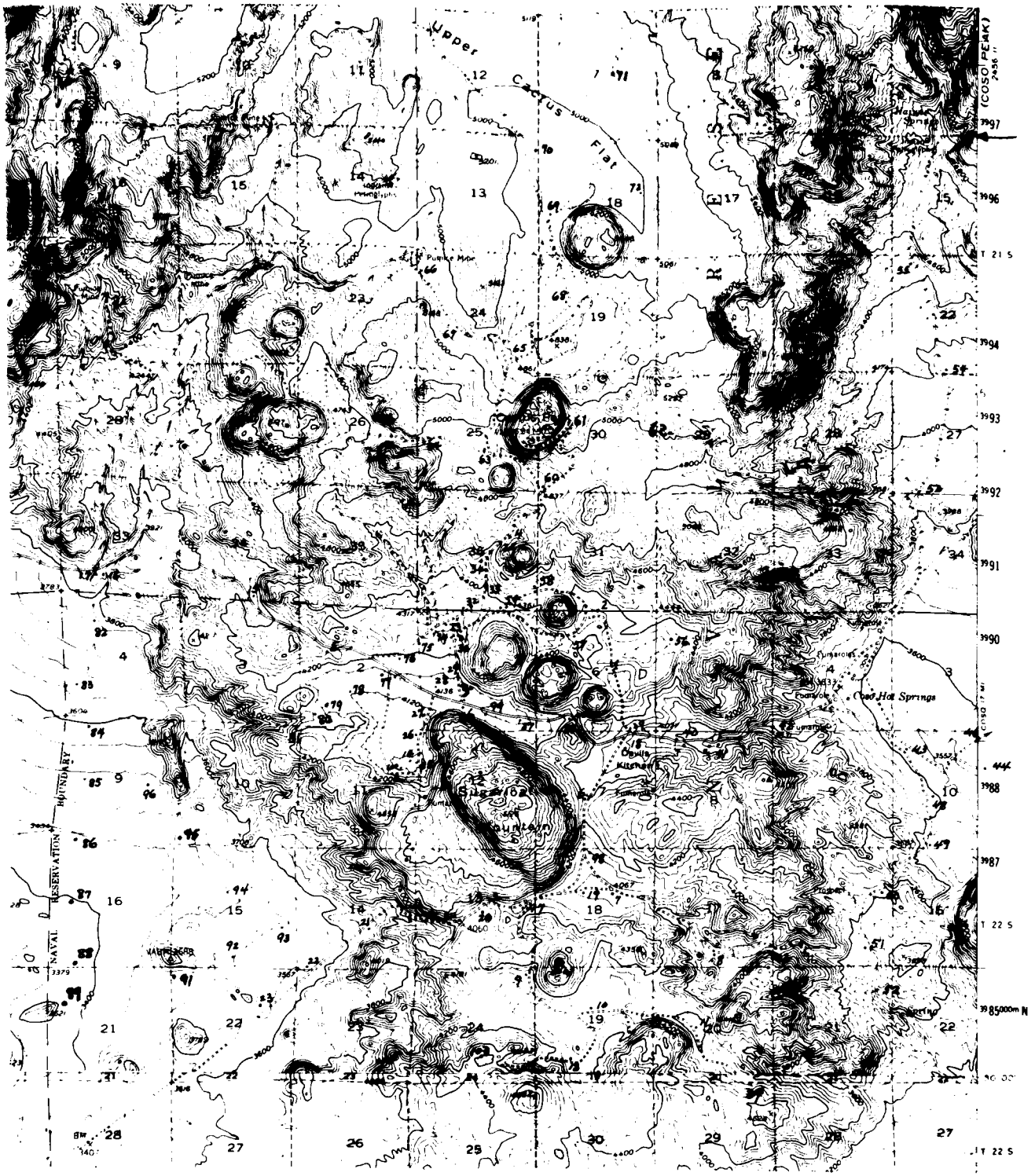

FIGURE 1: Locations of 2-m temperature stations at Coso. The first 24 were emplaced in July 1977, the rest in September 1977. (Haiwee Reservoir and Little Lake Quadrangles).

(c) Take soil sample for type determination.

(d) Measure surface roughness, surface albedo, thermal conductivity.

(e) After equilibration (2-4 days, depending on hole size) read thermistor probe. One reading will suffice.

(f) Using the annual wave correction program, calculate the normal 2-m temperature for the given location and time using the following inputs: 18-24 months of weather data (see Section 3.4.1) from nearest National Weather Service Station; thermal diffusivity (calculated from thermal conductivity); surface roughness and albedo. Output is normal 2-m temperature for given location and time.

(g) Subtract normal 2-m temperatures from observed 2-m temperatures to obtain residual geothermal anomaly.

With this as a guide, we have used the annual wave correction program (discussed in Section 3) to analyze our Coso 2-m temperature data by entering our surface effect parameters as follows:

- Surface Roughness: This was measured at Coso sites 1-24 according to the method of Lettau (1969). Photographs were taken at all 102 sites. The 24 measured sites had surface roughness values (Z_o) ranging from 0.1 cm to 16.1 cm. From the photographs, the range of these values appeared to be roughly representative of the remainder of the area. For the purpose of evaluating our correction model and reducing the number of individual computations, we divided surface roughness into four categories A-D: with A having a mean value of 3 cm; B having a mean value of 8 cm; C having a mean value of 12 cm; D having a mean value of 18 cm. From examination of the photographs of the measured sites, i.e., 1-24, we subjectively assigned the remaining sites into appropriate surface roughness categories.

- Thermal Diffusivity: Thermal diffusivity was measured at Coso using the phase lag method as described in LeSchack *et al* (1979). The values ranged from 0.0012 to 0.0025 cm^2/sec. As above, to reduce the number of computations, we divided the thermal diffusivity values into five categories as follows:

Category	Interval	Mean Thermal Diffusivity ($cm^2/sec.$)
1	.00120-.00146	0.0013
2	.00146-.00172	0.0016
3	.00172-.00198	0.00185
4	.00198-.00224	0.0021
5	.00224-.00250	0.0024

- Surface Albedo: As mentioned in LeSchack *et al* (1979), during preliminary evaluation of the annual wave correction model, variation of surface albedo from 25-40% had little noticeable effect on 2-m temperatures. We felt justified in using the mean value of 33% derived from the measurements at Coso sites 1-24. This was representative of the remainder of the Coso area.

3. The Annual Wave Correction Model

3.1 Introduction

The use of 2 meter temperatures for geothermal exploration is predicated on removal of the annual temperature wave which masks the geothermal signal. This annual effect must be mathematically specified or filtered from observed data before assessing the geothermal potential of a target region. At 2-m depths only the surface-induced annual temperature wave is of concern; transient waves are damped rapidly with depth, and for most soils the diurnal temperature pulse has little consequence at depths greater than 0.5 meters.

The partitioning of energy flux (radiant, sensible, evaporative, and soil) at the earth's interface is a function of meteorological and surface conditions. Meteorological parameters such as solar radiation and wind velocity, and surface conditions such as albedo and surface roughness, will determine the amount of energy propagated into the soil. Once the energy is conducted into the soil matrix, the physical properties of the soil will determine the magnitude and speed of propagation of the soil heat flux. Therefore, the soil's thermal diffusivity and conductivity properties, which are conditioned by mineral, water and air content, influence the amplitude and phase of the annual temperature wave at 2 meters.

We developed an annual surface climatic simulation model to account for the annual soil temperature wave, based on the work of Goodwin (1972). Given local monthly climatic parameters and surface/soil conditions, the model can reconstruct surface energy exchanges (sensible, latent and soil heat fluxes) and soil temperatures to a depth of 10 m.

Described below is the theoretical form of the surface energy budget simulation with a discussion of some of the model's underlying assumptions. The numerical schemes are outlined with emphasis on methods of constructing the

the soil's temperature profile. Also, details of the model's input and output will be specified.

3.2 Model Structure

3.2.1 Theoretical Basis of Model

The radiation balance for a particular surface (SFC) is expressed for clear skies conditions as:

$$Q^* = (1-\alpha)(Q+q) + \varepsilon\sigma T^4_{SKY} - \varepsilon\sigma T^4_{SFC} \quad (1)$$

where Q^* is net radiation.

α is albedo, Q+q is beam and diffuse solar radiation, respectively, σ is the Stefan-Boltzmann constant and ε is emissivity. For a complete description of this formulation, the reader should consult Sellers (1965), Oke (1978), and Montieth (1973). The sky radiation is estimated using the empirical Brunt equation:

$$\varepsilon\sigma T^4_{SKY} = T^4_{AIR}\ (a+b\sqrt{e}) \quad (2)$$

where a and b are empirical constants and e is vapor pressure of the air.

Using the assumption that the soil surface radiates essentially as a black body, equation (1) can be written as

$$Q^* = (1-\alpha)(Q+q) + \sigma T^4_{AIR}(a+b\sqrt{e}) - \sigma T^4_{SFC} \quad (3)$$

Since α, (Q+q), T_{AIR} and e are assigned as data, Q^* can be calculated explicitly as a function of surface temperature (T_{SFC}).

Equation (3) is for clear sky conditions. Variations in solar input induced by changing cloud cover are corrected by using percent clear sky and a correction factor for the cloud type following Sellers (1965). Equation (3) is rewritten as:

$$Q^* = (1-\alpha)(Q+q) + (\sigma T^4_{AIR}\ (a+b\sqrt{e}) - \sigma T^4_{SFC})\ (PCL+(1-PCL)CT)$$

where PCL is percent clear sky and CT = cloud cover correction factor.

The non-radiative components of the energy balance need to be specified to complete the total energy exchange at the earth's interface. The non-radiative transfers are:

$$Q^* = Q_H + Q_L + Q_S$$

where Q_H = sensible energy flux

Q_L = latent energy flux

Q_S = soil energy flux

The first two transfers of energy occur in the surface layer (a layer of the atmosphere up to approximately 10 m) by turbulent transfer, whereas soil heat flux occurs through a conductive process.

3.2.2 Sensible Energy Flux

Sensible heat is transported by turbulent eddies which are a function of the stability regime of the lower atmosphere. Therefore, any expression describing sensible energy transfer must incorporate a stability-dependent function. The annual simulation model uses the Businger-Dyer (Businger, 1971; Dyer, 1967) formulation for calculation of sensible energy flux in the surface layer. An assumption that is characteristic of all surface layer calculations is that the energy flux is constant throughout this layer.

The stability of the surface layer is determined by the Richardson number:

$$Ri = g \frac{\partial \bar{\theta}}{\partial z} \Big/ \bar{\theta} \left(\frac{\partial \bar{U}}{\partial z}\right)^2 \qquad (6)$$

where g is acceleration due to gravity

θ is the mean potential temperature

z is the vertical coordinate

U is the magnitude of the mean horizontal wind vector

The Ri number is a dimensionless quantity which varies from less than -0.025 for a free convective regime, to greater than -0.025 and less than 0 for forced convection, where zero defines the neutral condition; from >0 to <0.4 is a stable state; and finally values for Ri number >.4 define a laminar condition where essentially all turbulent motion is suppressed.

Under neutral atmosphere conditions the mean wind flow is logarithmic with height as

$$\frac{\partial \bar{U}}{\partial z} = U^*/kz \qquad (7)$$

where U* is friction velocity and k is the von Karman constant. If equation (7) is integrated from some reference height Z_o, (Z_o) = surface roughness) one obtains

$$\bar{U} = U^*/k \ln\left(\frac{z}{z_o}\right) \tag{8}$$

If Z_a is the instrument height and $\bar{U}$ is the mean wind speed from Z_o (U = o) to Z_a,

then $$U^* = k\bar{U}/\ln\left(\frac{Z_a}{Z_o}\right) \tag{9}$$

U* is a scaling parameter for the wind.

Similarly, from

$$\frac{\partial\theta}{\partial z} = \Theta^*/z \tag{10}$$

where Θ* is a scaling temperature,

$$\Theta^* = (\Theta_{za} - \Theta_o)/\ln\left(\frac{Z_a}{Z_o}\right) \tag{11}$$

Now the sensible heat flux can be calculated by

$$Q_H = \rho c k U^* \Theta^* \tag{12}$$

where ρc = volumetric heat capacity of air; ρ = air density and c = specific heat.

Under non-neutral conditions Equations (9) and (11) are modified

$$U^* = k\bar{U}/(\ln\left(\frac{Z_a}{Z_o}\right) - \psi_1) \tag{13}$$

$$\Theta^* = (\Theta_{za}-\Theta_o) \ /\ln\left(\frac{Z_a}{Z_o}\right) - \psi_2) \tag{14}$$

where ψ_1 and ψ_2 are functions of atmospheric stability (Paulson, 1970).

From the original work of Businger (1971) and Dyer (1967), Paulson shows that ψ_1 is computed for unstable conditions by

$$\psi_1 = 2 \ln\left[(1+x)/2\right] + \ln\left[(1+x^2)/2\right] - 2 \tan^{-1}x + \frac{\pi}{2} \tag{15}$$

where

$$x = (1 - \gamma \frac{z}{L})^{\frac{1}{4}} \tag{16}$$

γ is an empirical constant and z/L is a stability function such that

$$Ri = Zm/L$$

where Zm is geometric mean height and L is the Obukov length given by

$$L = - U^{*3}cT/kgQ_H.$$

For temperature stability correction the following expression is used

$$\psi_2 = 2 \ln \left[(1 + x^2)/2\right] \quad (17)$$

Under stable conditions,

$$L = Zm\ (1 - 7Ri)/Ri \quad (18)$$

and

$$\psi_1 = \psi_2 = 7\left(\frac{z}{L}\right) \quad (19)$$

When Ri = 0 (neutral conditions), the stability parameters (ψ_1 and ψ_2) are equal to zero.

3.2.3 Latent Energy Flux

The transfer of latent energy is obtained by using the Bowen ratio in conjunction with Equation (12). The Bowen ratio is an expression of energy partition between sensible and latent energy flux

$$B = \frac{Q_H}{Q_L} \quad (20)$$

Q_H and Q_L can be written in terms of a gradient relationship as follows:

$$Q_H = \rho c K_H \frac{\partial \theta}{\partial z} \quad (21)$$

and

$$Q_L = \rho L K_L \frac{\partial q}{\partial z} \quad (22)$$

where ρ is air density, L is latent heat of vaporization, q is specific humidity and K_H and K_L are the eddy diffusivity for heat and moisture respectively.

Dividing Equations (21) and (22) one obtains the Bowen ratio

$$B = \frac{Q_H}{Q_L} = \frac{\rho c K_H \left(\frac{\partial \theta}{\partial z}\right)}{\rho L K_L \left(\frac{\partial q}{\partial z}\right)} \simeq \frac{c}{L} \frac{(\theta_2 - \theta_1)}{(q_2 - q_1)} \frac{K_H}{K_L} \tag{23}$$

if $K_H = K_L$, which is the general assumption, then

$$Q_L = \frac{Q_H L (q_2 - q_1)}{c(\theta_2 - \theta_1)} \tag{24}$$

Serious questions remain as to the legitimacy of long term arithmetric mean values in the computation of average Richardson numbers and energy fluxes at time scales considered in this model. It remains to be tested as to the physical reality of these assumptions.

3.2.4 Soil Energy Flux

Soil heat flux is related to the time rate of change of the soil heat content by,

$$Q_s = \frac{\partial H}{\partial t} \tag{25}$$

The heat content for a column of soil at depth z and unit area is

$$H = \rho c z \bar{T} \tag{26}$$

T is mean temperature of the soil. Setting Equation (25) equal to the time rate change of temperature produces

$$Q_s = \frac{\partial H}{\partial t} = \rho c z \frac{\partial T}{\partial t} \tag{27}$$

The flow of heat into the soil can also be given by

$$Q_s = k \frac{\partial T}{\partial t} \tag{28}$$

where k is thermal conductivity of the soil.

Then

$$\frac{\partial Q_s}{\partial z} = \rho c \frac{\partial T}{\partial t} = \frac{\partial}{\partial z}\left(k \frac{\partial T}{\partial z}\right) \tag{29}$$

When k is constant with depth, the Fickian diffusion equation is obtained by restructing Equation (29) to produce

$$\frac{\partial T}{\partial t} = \frac{k}{\rho c}\left(\frac{\partial^2 T}{\partial z^2}\right) = \alpha_s \left(\frac{\partial^2 T}{\partial z^2}\right) \tag{30}$$

α_s is the soil thermal diffusivity

The solution of Equation (30) for equally spaced nodes is the method for obtaining the time history of soil temperatures given a periodic surface forcing function. Q_s is calculated from Equation (29) after the temperature distribution is computed.

In a desert region, such as Coso, it is assumed that convection of heat by percolating water in the soil is small, especially averaged over 5 days, and that no freeze-thaw phase changes occur. In addition, a major assumption of the model at the specified time scale is that mean temperature profiles in the soil over a five-day period are linear.

3.3 Numerical Scheme

The finite difference equations are developed for the Richardson number, sensible energy and latent energy fluxes. (See Goodwin, 1972 and Outcalt 1972). The Fickian diffusion Equation (30) is developed in the finite form utilizing a back differencing method. The temperature at depth Z_N in the soil at time increment I is given by

$$T_N(I) = T_N(I-1) + \alpha_s \frac{\Delta t}{(\Delta z)^2}\left[T_N\text{-}1(I-1) - 2_N(I-1) + T_{N+1}(I-1)\right] \tag{31}$$

where T_{N+1} is the temperature at some depth $Z_{N+1} > Z_N$, α_s is soil thermal diffusivity, t and z are the time increment and depth increment respectively. This Equation is solved for 10 nodal points with Δz equal to 1 meter and Δt equal to 4.32×10^5 seconds (or 5 days). The quantity $\left(\alpha_s \frac{\Delta t}{\Delta z^2}\right)$ has very interesting properties and is referred to as the Fourier modulus. This modulus can be used to determine the computational stability of Equation (31). The stability criterion is

$$0 < \alpha_s \frac{\Delta t}{(\Delta z)^2} < \tfrac{1}{2} \tag{32}$$

The numerical solution of Equation (30) for equally spaced nodes is stable (real) only if the above condition is satisfied. Inserting the range of values for soil thermal diffusivity and the time-depth increments, the stability criterion is always satisfied within the context of the Coso simulation. The finite difference equation for soil heat flux at time I is then

$$Q_S(I) = k(T_2 - T_{SFC})/\Delta z \qquad (33)$$

The complete numerical solution for the model at a particular time step hinges on the specification of all the variables needed to calculate the components of surface energy transfer on the meteorlogical (M) and surface (G) based data. The four components of surface energy transfer are net radiation (Q*) and the soil (Q_S), sensible (Q_H), and latent (Q_L) heat fluxes. These can be specified as transcendental in surface temperature (T) in the familiar energy conservation equation,

$$Q^*(G,M,T) + Q_S(G,T) + Q_H(G,M,T) + Q_L(G,M,T) = 0 \qquad (34)$$

An interval halving algorithm is selected to carry out a search for that temperature which will drive the above equation to a zero sum condition. Thus, at each iteration, the surface temperature and all of the components of surface energy transfer are outputs in addition to the substrate (soil) temperature profile (Pease, *et al*, 1976).

3.4 Input and Output of the Annual Model

3.4.1 Input

The annual energy budget simulation model requires six data parameters and 15 mean monthly values for each of the eight data variables.

The parameters include:

- Soil properties;
- climatological properties;
- numerical node constants for the model.

Data variables are:

- Climatological variables;
- surface characteristics.

The soil properties needed as input are thermal conductivity and diffusivity. Thermal diffusivity (cm^2/sec) is

obtained by measuring the temperature amplitude decrease with depth or temperature phase change with time.

The two climatological parameters are ground temperature mean (^{o}F) for the 15 monthly temperature values and a cloud-type correction factor which modifies effective outgoing radiation values, as specified in Sellers (1965). The node spacing for the soil was tested for numerical stability and a value of 100 cm was found satisfactory. The instrument shelter height of 150 cm was used as the atmosphere's upper boundary condition. These parameters remain constant for the 15 month test period and for each site location.

The two sets of data variables consist of five climatological and three surface cover variables. These variables are submitted to a Fourier mathematical smoothing routine which computes a value for each variable at 91 time steps, producing five-day equally-spaced data points over the 15-month period. The input climatological variables are:

- Mean monthly dew point (^{o}F);
- mean monthly percent clear skies (%);
- mean monthly atmospheric pressure (corrected to mean elevation of 4127 ft.) (in. Hg);
- mean monthly air temperature (^{o}F);
- mean monthly wind speed (mph).

These variables were obtained from the China Lake Naval Weather Station located 25 miles south of Coso between January 1977 to March 1978. These values are considered uniform over an extensive area, justifying their extrapolation to the Coso region. Table 1 shows the mean monthly climatological input.

The surface characteristics values are:

- Surface aerodynamic roughness (cm);
- surface relative humidity (%);
- surface reflectivity-albedo (%).

The aerodynamic roughness is calculated from measured geometric properties of the surface following techniques outlined in Lettau (1969). The surface relative humidity is defined as the percent of wet fraction which is determined by the soil moisture content in the upper horizon. The

TABLE 1: INPUT CLIMATOLOGY; WEATHER DATA FROM THE U.S. NAVAL WEAPONS CENTER, CHINA LAKE, CALIFORNIA

1977	Temperature (^{o}F)	Dew Point (^{o}F)	Wind Speed (MPH)	Pressure (in Hg)	Skycover %
January	44.59	24.85	3.74	27.71	4.52
February	52.46	20.57	3.96	27.76	4.12
March	50.45	16.55	6.66	27.60	2.66
April	65.41	24.28	4.06	27.60	3.53
May	64.08	32.82	7.32	27.51	3.83
June	83.9	40.13	5.73	27.53	3.45
July	87.88	35.62	6.2	27.57	1.54
August	85.9	43.83	5.82	27.53	2.51
September	77.5	38.27	5.63	27.54	2.3
October	68.55	31.29	3.68	27.63	2.52
November	56.4	18.93	4.7	27.68	4.45
December	50.60	28.48	3.35	27.69	5.02
1978					
January	47.79	35.65	3.05	27.69	6.16
February	51.75	33.55	4.18	27.62	5.45
March	58.44	38.97	5.21	27.62	6.03
Mean	65.6				

third variable, albedo, is the ratio of reflected solar radiation to the total incoming solar (global)* radiation. Albedo and surface roughness were measured at 24 individual field sites. Surface relative humidity was calculated from soil samples taken at these same locations. The soil samples were sealed in double plastic bags and sent to a laboratory for analysis. Once a surface characteristic was determined, it was assumed constant for a given site over the 15 month period for which meteorological data were gathered. Given the arid/semi-arid nature of the test location, we feel this assumption is correct.

In addition to these specified initial conditions, the model also generates three internal variables. It transforms the dew point temperatures to air vapor pressures; it calculates sky radiant temperature from atmospheric temperature, atmospheric moisture, and the cloud correction factor; and it has an attached solar radiation generator**, which calculates mean 5-day global radiation values corrected for changing sky cover conditions.

3.4.2 Output

The model output consists of 5-day interval values for sensible, latent, soil heat flux, and net radiation. At each time step, a soil temperature profile is printed consisting of temperatures at a 1 m node spacing down to a depth of 10 meters.

4. Evaluating the Annual Wave Correction Model

To evaluate the Annual Wave Correction Model according to step (f) in Section 2, and obtain the residual geothermal anomaly in step (g), we would be required to make 102 computations of normal temperatures at 2-m depths. However, since the main input variables for each site, i.e., surface roughness and thermal diffusivity, appeared repetitive in various combinations, we divided both variables into four surface roughness categories and five thermal diffusivity categories, as discussed above. Each site was given a surface roughness-thermal diffusivity classification; they are listed along with the September, 1977 temperatures corrected for elevation, in Table 2. Table 3 shows the various combinations. Using this technique, we reduced the number of computations from 102 to 17. In view of the uncertainties in the model and the input data, a larger range of classifications with an increase in number of computations was not considered justifiable.

Using the 17 sets of input variables shown in Table 3,

*Global radiation is the sum of direct and diffuse radiation on a horizontal surface.
**John Davies of McMaster University provided the bases for this solar radiation routine.

TABLE 2: TEMPERATURE, THERMAL DIFFUSIVITY, ROUGHNESS/DIFFUSIVITY GROUP, COMPUTED NORMAL TEMPERATURES, AND RESIDUALS FOR COSO KGRA

Station[1]	Temp. °C[2] (Sept 1977)	Thermal[3] Diffusivity	Thermal Diffusivity/[4] Surface-Roughness Class	Computed Temp. °C	Residual °C
1	27.0	1.62	2B	23.7	3.3
2	25.5	1.51	2B	23.7	1.8
3	26.0	1.31	1B	22.6	3.4
4	27.0	1.62	2A	24.8	2.2
5	27.7	2.27	5B	25.8	1.9
6	33.2	1.22	1B	22.6	10.6
7	30.1	1.51	2B	23.7	6.4
8	26.2	1.62	2B	23.7	2.5
9	27.3	1.51	2C	23.3	4.0
10	25.7	1.75	3A	25.6	0.0
11	26.7	1.75	3B	24.4	2.2
12	25.3	1.62	3D	23.0	2.3
13	25.8	1.75	3B	24.4	1.4
14	23.5	1.62	2A	24.8	-1.3
15	25.6	1.62	2C	23.3	2.3
16	26.3	1.91	3A	25.6	0.7
17	26.7	2.27	5A	27.0	-0.3
18	28.6	1.75	3B	24.4	4.2
19	29.4	1.51	2B	23.7	5.7
20	26.1	1.40	1B	22.6	3.5
21	26.3	1.75	3B	24.4	1.9
22	25.0	1.62	2C	23.3	1.7
23	25.1	1.62	2B	23.7	1.4
24	25.7	1.91	3B	24.4	1.3
25	23.5	1.22	1C	22.2	1.3
26	26.0	1.62	2A	24.8	1.2
27	25.0	1.40	1B	22.6	2.4
28	25.7	1.91	3C	24.1	1.6
29	25.9	1.62	2B	23.7	2.2
30	26.7	1.40	1A	23.6	3.1
31	26.5	1.40	1B	22.6	3.9
32	26.7	1.40	1D	21.9	4.8
33	28.8	1.91	3C	24.1	4.7
34	26.5	1.40	1B	22.6	3.9
35	26.0	1.51	2B	23.7	2.3
36	25.4	1.91	3D	23.7	1.7
37	26.9	1.62	2D	23.0	3.9
38	28.0	1.62	2D	23.0	5.0
39	29.1	1.51	2B	23.7	5.4
40	31.7	1.31	1B	22.6	9.1
41	33.3	1.91	3C	24.1	9.2
42	31.2	2.07	4C	24.7	6.5
43	25.0	1.75	3B	24.4	0.6
44	23.1	1.62	2C	23.3	-0.2
45	23.6	2.07	4B	25.1	-1.6
46	24.7	2.48	5B	25.8	-1.1
48	24.8	1.91	3B	24.4	0.4
49	25.3	2.07	4B	25.1	0.2
50	29.9	1.62	2A	24.8	5.1
51	30.8	1.62	2B	23.7	7.1
52	33.8	2.27	5A	27.0	6.8
53	25.1	1.75	3B	24.4	0.7
54	26.2	1.91	3B	24.4	1.8
55	28.0	2.27	5A	27.0	1.0
56	28.3	1.62	2A	24.8	3.5
57	26.9	1.40	1C	22.2	4.7
58	27.6	1.62	2B	23.7	3.9
59	26.7	1.62	2C	23.3	3.4
60	26.7	1.40	1B	22.6	4.1
61	27.0	1.40	1A	23.6	3.4
62	26.1	1.62	2C	23.3	2.6
63	26.7	1.51	2A	24.8	1.9
64	26.3	1.62	2A	24.8	1.5
65	24.7	1.62	2A	24.8	-0.1
66	25.0	1.75	3A	25.6	-0.6
67	25.2	1.62	2A	24.8	0.4
68	23.8	1.62	2A	24.8	-1.0
69	23.1	1.40	1A	23.6	-0.5
70	24.3	1.75	3B	24.4	-0.1
71	25.7	1.62	2B	23.7	2.0
72	24.9	1.40	1A	23.6	1.3
73	26.9	1.62	2A	24.8	2.1
74	26.6	1.75	3A	25.6	1.0
75	24.9	1.40	1C	22.2	2.7
76	25.6	1.22	1B	22.6	3.0
77	25.7	1.51	2B	23.7	1.9
78	25.6	1.62	2B	23.7	1.9
79	26.6	1.75	3B	24.4	2.2
80	26.6	1.75	3A	25.6	1.0
81	25.4	1.51	2A	24.8	0.6
82	26.8	1.91	3A	25.6	1.2
83	25.7	1.75	3C	24.1	1.6
84	25.2	1.90	3B	24.4	0.8
85	24.7	1.75	3A	25.6	-0.9
86	24.5	1.75	3A	25.6	1.1
87	24.3	1.62	2B	23.7	0.6
88	23.2	1.75	3A	25.6	-2.4
89	23.5	1.75	3B	24.4	-0.9
90	23.7	1.91	3B	24.4	-0.7
91	24.1	1.91	3B	24.4	-0.3
92	24.1	1.91	3B	24.4	-0.3
93	25.1	2.07	4A	26.3	-1.2
94	23.8	1.51	2B	23.7	0.1
95	24.7	1.91	3B	24.4	0.3
96	24.8	1.91	3A	25.6	-0.8
97	27.2	1.31	1B	22.6	4.6
98	30.2	1.22	1A	23.6	6.6
99	25.6	1.51	2D	23.0	2.6
100	25.3	1.62	2D	23.0	2.3
101	26.7	1.40	1A	23.6	3.1
102	26.0	1.51	2B	23.7	2.3
103	26.3	1.40	1B	22.6	3.7

NOTES: [1]No data were taken at Station #47.

[2]Temperature values in (°C) have all been corrected for elevation differences. Corrections based on an adiabatic lapse rate of -1.0°C/100 m. Corrections are keyed to an arbitrarily picked datum of 3400 ft elevation (See LeSchack *et al* (1977).

[3]Thermal diffusivity is expressed in cm^2/sec.

[4]Surface roughness (A-D) and thermal diffusivity classes (1-5) were determined according to procedures discussed in Section 2 above.

TABLE 3: SURFACE ROUGHNESS/THERMAL DIFFUSIVITY COMBINATIONS AND OTHER MODEL INPUT VALUES

SURFACE ROUGHNESS CLASS (cm) \ THERMAL DIFFUSIVITY CLASS (cm^2/sec)	1	2	3	4	5
A	0.0013 3	0.0016 3	0.00185 3	0.0021 3	0.0024 3
B	0.0013 8	0.0016 8	0.00185 8	0.0021 8	0.0024 8
C	0.0013 12	0.0016 12	0.00185 12	0.0021 12	
D	0.0013 18	0.0016 18	0.00185 18		

OTHER INPUT VARIABLES

(1) Mean albedo; 0.33

(2) Mean percentage moisture; 0.05

(3) Volumetric heat capacity (ρcp); 0.4

TABLE 4: COMPUTED NORMAL TEMPERATURES FOR 17 SETS OF MODEL INPUT DATA BASED ON SURFACE ROUGHNESS/THERMAL DIFFUSIVITY CLASSES, TEMPERATURES IN ^{o}C

SURFACE ROUGHNESS CLASS \ THERMAL DIFFUSIVITY CLASS	1	2	3	4	5
A	23.6	24.8	25.6	26.3	27.0
B	22.6	23.7	24.4	25.1	25.8
C	22.2	23.3	24.1	24.7	
D	21.9	23.0	23.7		

we chose to evaluate the model for data gathered during 22-24 September, 1977, because at this time of year the 2 m temperatures are close to their peak annual value. This results in maximum temperature contrast between areas of low and high thermal diffusivity. The computed normal temperatures are shown in matrix form in Table 4.

5. Preparing the Residual Map

In theory, if there is no anomalous geothermal heat flux, the evaluation of the Annual Temperature Correction Model at each site for a given date should produce a 2-m temperature value equal to that actually measured for the same data. Any measured temperature greater than that computed by the model could be assumed to be caused by higher than normal heat flow. Values for the site, the roughness-diffusivity group, the measured temperature for September, 1977, corrected for elevation, and the computed temperatures are listed in Table 2. The differences between the measured values minus the computed values, i.e., the residuals, are also tabulated. When these residuals are contoured in the same fashion as the mean annual temperature map for Coso, and the two are compared as in Figures 2 and 3, the similarity can be seen. In short, the same map that was developed using a year's temperature data can be duplicated in much less time using temperatures recorded at a given time along with appropriate corrections derived from simultaneous ancillary data.

6. A Preliminary Test of the Model's Reliability

Because the model has not yet been refined to the maximum, and because there is uncertainty in the accuracy of our input data, we have evaluated on a statistical basis the reliability of our simulated normal temperatures. Using the residual map as a guide, we chose two areas: the southwest and the north where there are a number of data points and geothermal heat flow appears to be normal. At each site we compared the observed temperatures with their respective computed temperatures using the Student-T test, a statistical test for comparing data populations. The values are listed in Table 5. At both areas we can accept the null hypothesis that there is no significant difference between the means at the 5% level; there is a 95% probability that the computed and measured values come from the same population. If this is so, it suggests that the residual values for the entire Coso area are probably accurate to $+ 1.9^{o}C$, based on the summation of the standard deviation of $\mp 0.96^{o}C$ for the observed temperatures corrected for elevation with the standard deviation of $+ 0.94^{o}C$ for the associated computed values, in the non-anomalous areas.

As the model is refined with further use, greater accuracy is expected. Although the present accuracy is adequate for the strong anomaly found at Coso, the true test will come when the Annual Wave Correction Model is applied to an area where the temperature anomaly is much less.

FIGURE 2: (Above) Mean annual temperature contour map for Coso, corrected for elevation. Temperatures in ^{o}C.

FIGURE 3: (Right) Residual temperature contour map for Coso in ^{o}C. Residuals were prepared by subtracting normal 2-m temperatures computed from Annual Wave Correction Model for 22-24 September 1977 from 2-m temperatures observed during this same period. Note close similarity between mean and residual anomaly patterns.

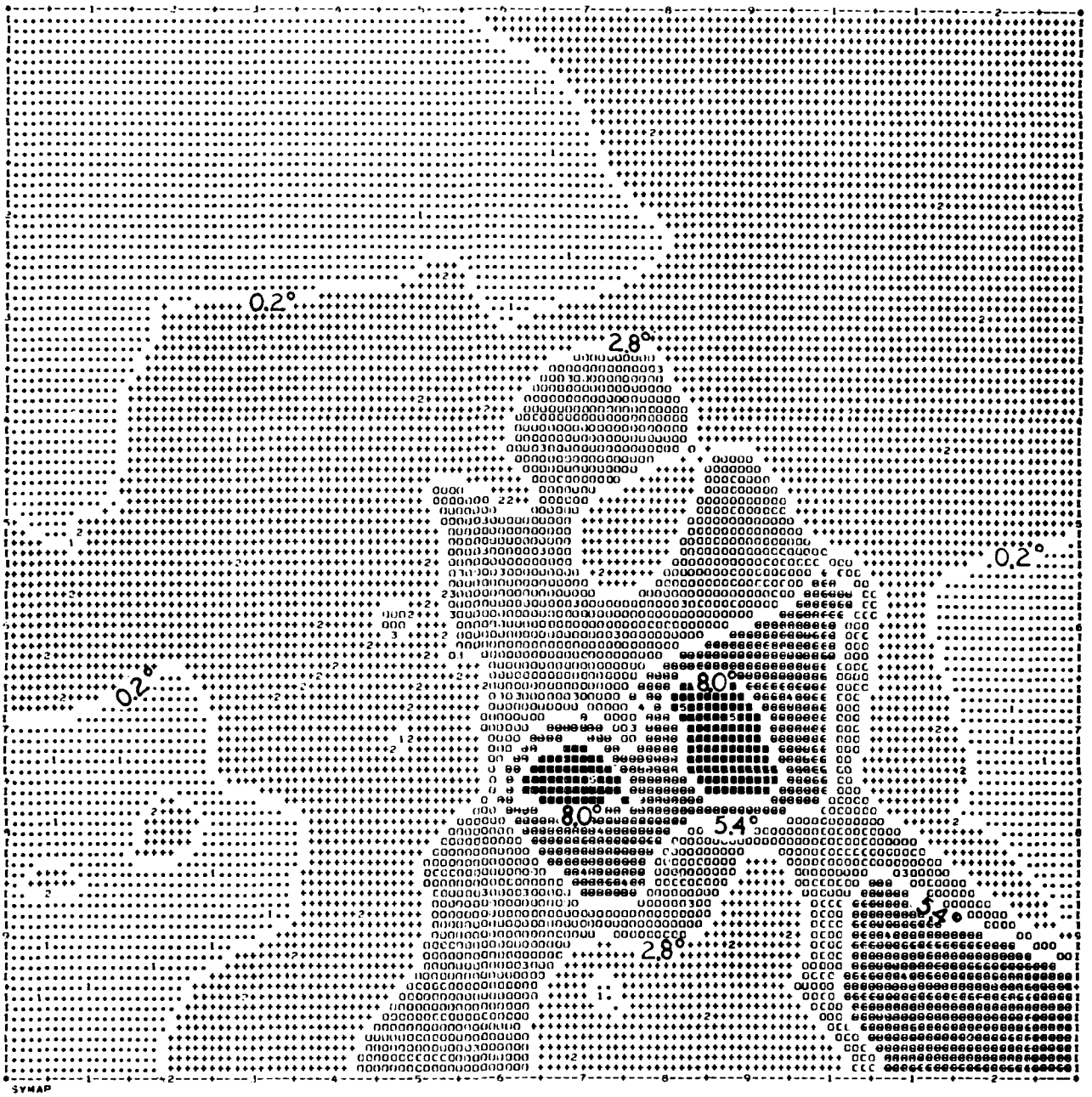
0.2°
2.8°
0.2°
0.2°
8.0°
8.0°
5.4°
2.8°
SYMAP

TABLE 5: A COMPARISON OF SEPTEMBER 1977 TEMPERATURES, RECORDED AT TWO NON-ANOMALOUS AREAS AT COSO AND CORRECTED FOR ELEVATION, WITH TEMPERATURES COMPUTED FOR THE SAME SITE AND TIME WITH THE ANNUAL WAVE CORRECTION MODEL

Station	WEST Temperature °C	
	observed	computed
16	26.3	25.6
17	26.7	27.0
22	25.0	23.3
23	25.1	23.7
82	26.8	25.6
83	25.7	24.1
84	25.2	24.1
85	24.7	25.6
86	24.5	25.6
87	24.3	23.7
88	23.2	25.6
89	23.5	24.4
90	23.7	24.4
91	24.1	24.4
92	24.1	24.4
93	25.1	26.3
94	23.8	23.7
95	24.7	24.4
96	24.8	25.6

Computed T value = 0.03187

Station	NORTH Temperature °C	
	observed	computed
65	24.7	24.8
66	25.0	25.6
67	25.2	24.8
68	23.8	24.8
69	23.1	23.6
70	24.3	24.4
71	25.7	23.7
72	24.9	23.6

Computed T value = 0.44926

STD of computed values = ±0.94

STD of observed values = ±0.96

7. Examining the Effect of Topography on Shallow Isotherms

We have studied the effect of topography on sub-surface isotherms at Coso KGRA using a model (FINITEG) developed by Lee (1977). The model was used to predict sub-surface temperatures to a depth of 0.75 km in the area of Cactus Peak (Figure 1). Program FINITEG uses the finite-element method to develop a numerical temperature grid within specified boundaries so that isotherms can be drawn. When these isotherms are superimposed on a topographic profile of the area, it can be determined if the isotherms conform to the topographic profile. Conformity is necessary for a survey in an area of significant topographic relief, such as Coso.

The FINITEG program can provide solutions for steady-state or transient conditions. It allows for the addition of anomalous areas to the data set to provide a more realistic geological model of heat flow problems. FINITEG provides steady state or transient solutions for a number of heat flow conditions that can be related to relief, heat generation, erosion, sedimentation, igneous intrusion, non-uniform surface temperature, transient surface temperature and inhomogeneous thermal properties. The model allows for the treatment of a single situation or a combination of them.

We have used the variable relief and inhomogeneous thermal property features to model an east-west transect through Cactus Peak, an area which appears to have normal heat flow. Figure 4 illustrates the physical construction of the model, the details of which are discussed in the Appendix. Using values determined from field measurements, we have evaluated the model and have developed the thermal structure illustrated in Figure 5.

This model has taken into account 100 m of topographic relief and the effects of three anomalous regions near the surface (representing the soil in which the measurements were made, as opposed to the more conductive bedrock). It is apparent from examination of Figure 5 that, within the resolution of the model, the isotherms conform to the topography. The contour interval is essentially unvarying as it approaches the surface, even though the isotherms pass through thin soil layers of different thermal conductivity. Our interpretation, from evaluating the Lee FINITEG model, is that in geological settings in the Basin and Range province, where there is some topographic relief and 2-m temperature measurements are made in a thin soil layer overlying a more conductive bedrock, there are no significant distortions to a 2-m temperature contour map because of either topography or soil thickness variations. We therefore feel confident to emplace our 2-m survey holes with little concern for topography or modest variations in soil conditions.

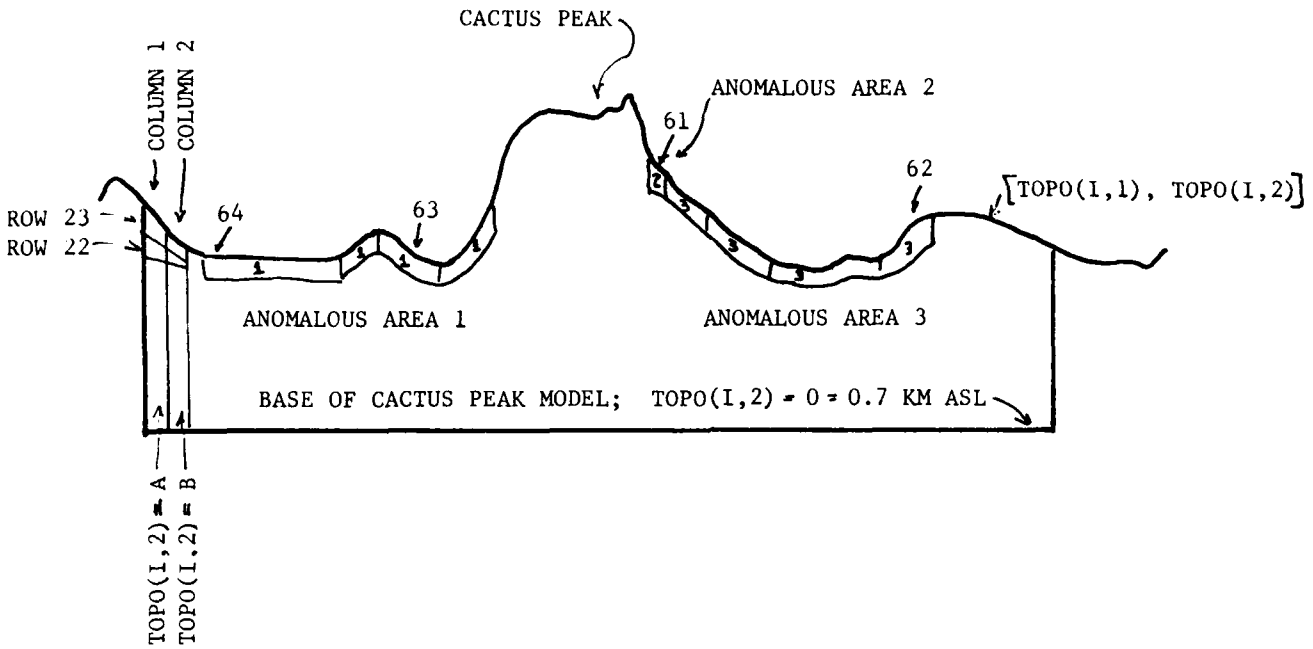

FIGURE 4: The physical construction of the 7.2 km transect through the Cactus Peak area. The upper boundary of the model is determined by the topographic profile. Cactus Peak is at an elevation of 5360 ft (1.63 km) or 0.93 km above the arbitrarily chosen base at 0.7 km above sea level. In the model, the number of rows per column is constant; owing to topographic variations, row thickness varies from column to column as shown in the case of rows 22 and 23.

8. Conclusions

In previous work we concluded that the steps essential to a SHALLO-TEMP™ survey were:

(a) At each site drill two adjacent 2-m holes;

(b) insert thermistor probe in one, thermal conductivity probe in the other;

(c) take soil sample for type determination;

(d) measure surface roughness, surface albedo, thermal conductivity.

(e) After equilibration (2-4 days, depending on hole size), read thermistor probe. One reading will suffice.

(f) Using the annual wave correction program, calculate the normal 2-m temperature for the given location and time using the following inputs: 18-24 months of weather (see section 3.4.1) from nearest National Weather Service Station; thermal diffusivity (calculated from thermal conductivity), and surface roughness and albedo. Output is normal 2-m temperature for given location and time.

(g) Subtract normal 2-m temperatures from observed temperatures to obtain residual geothermal anomaly.

In this work we have gleaned the soil and surface data required to conduct the survey at the Coso KGRA from previously discussed measurements or analyses. The meteorological data were obtained from NOAA weather records. An annual wave model was constructed and normal 2-m temperatures were calculated for each of our 2-m sites for the September, 1977, period. These normal temperatures were subtracted from the 2-m temperatures observed at each of the sites in September, 1977. A residual map was prepared. Anomalies derived from the residual map compared favorably with those interpreted from a mean annual 2-m temperature map for the same area. Using statistical techniques, we determined that the accuracy of the residual map produced by the SHALLO-TEMP™ method is $\pm$ 1.9°C. This may be improved with further refinement. However, we conclude the model is adequate for investigating anomalies of the magnitude found at Coso.

We have also used a mathematical model to evaluate the effect of topographical variations and near-surface variations

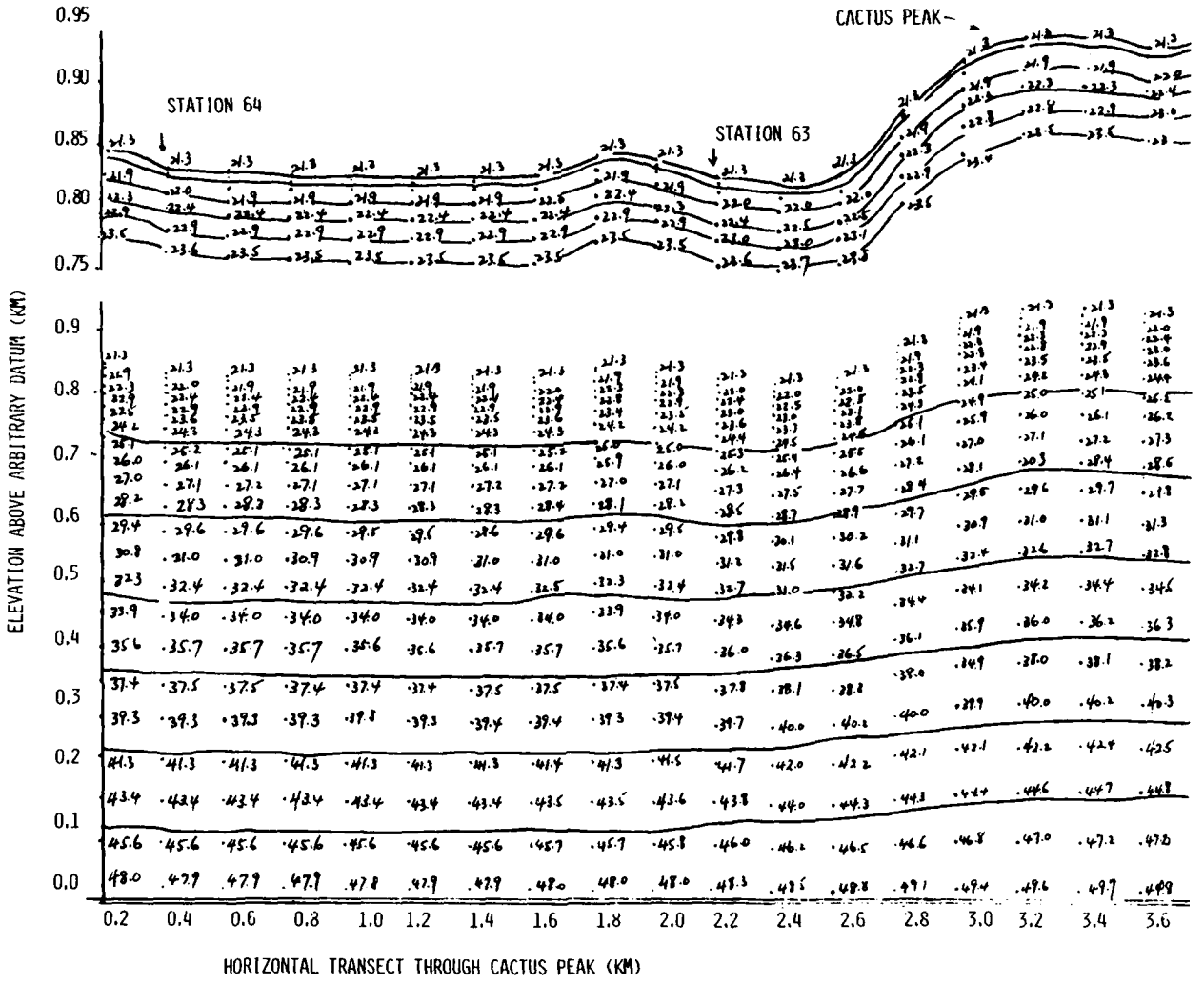

FIGURE 5: Output of the Lee FINITEG Model is plotted above for a 7.2 km East-West transect through Cactus Peak at the Coso KGRA. The upper 200 m of the vertical transect is shown in an expanded view at the top of the Figure. See text and Appendix A for details. Isotherms in ^{o}C.

VERTICALLY EXPANDED VIEW OF UPPER 200M OF TRANSECT

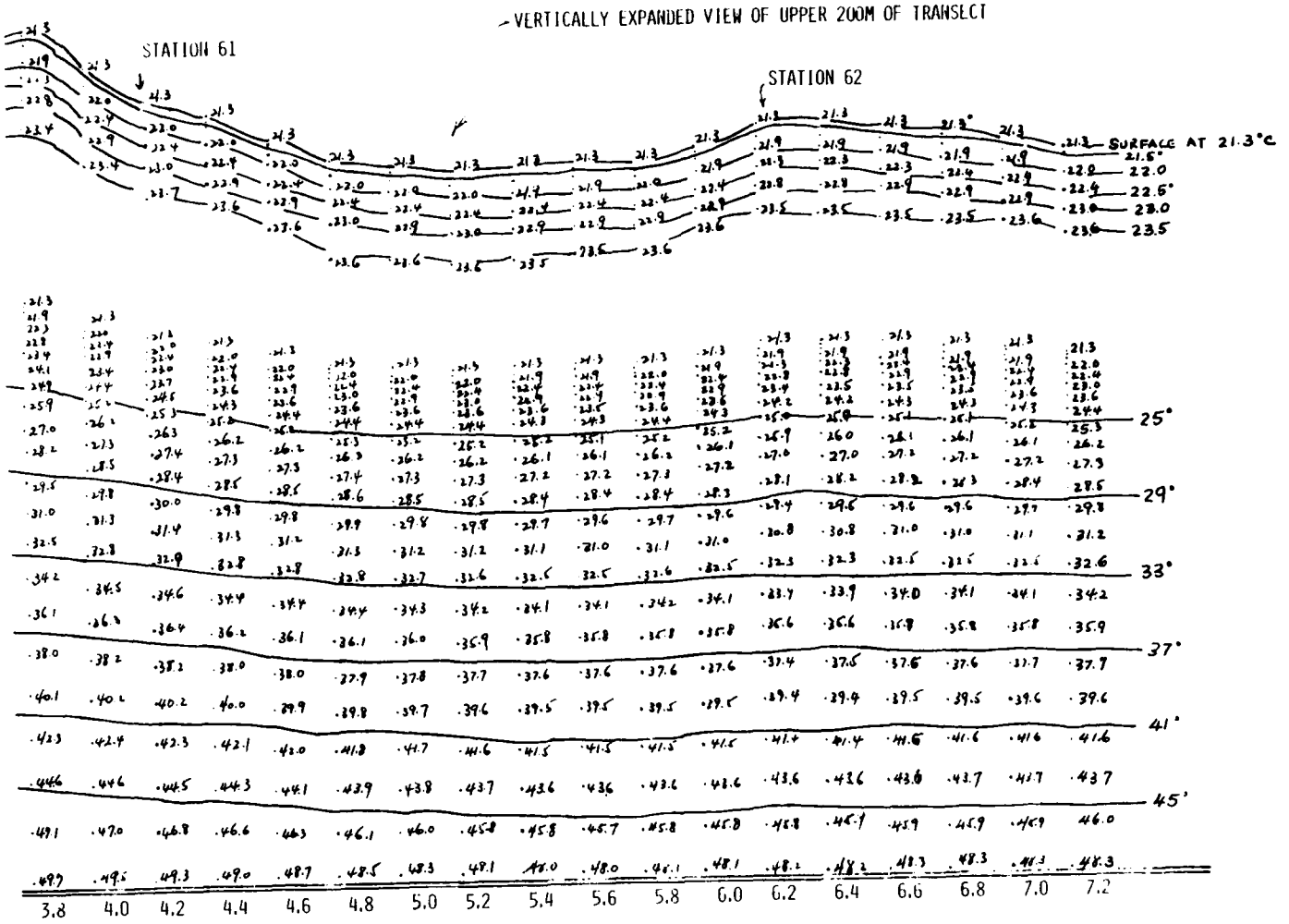

of geology on isotherms in a non-anomalous area of Coso, near Cactus Peak. Because the computed near-surface isotherms closely follow the surface topographical profile, we can confidently emplace our 2-*m* survey holes with relatively little concern for site location, if the water table is deep, as it is at Coso.

9. References

Businger, J.A. *et al*, 1971: Flux profile relationship in the atmospheric surface layer. J. Atmos. Sci., 28, 181-189.

Dyer, A.J., 1967: The turbulent transport of heat and water vapor in an unstable atmosphere. Quant. Ray. Meteor. Soc., 93, 501-508.

Goodwin, Cecil, 1972: Annual Active-Layer Simulator for Permafrost Regions, M.S. Thesis, University of Michigan, Ann Arbor, unpublished.

Lee, Tien-Chang, 1977, Application of Finite Element Analysis to Terrestrial Heat Flow, UCR/IGPP-77/15, Inst. of Geophs. and Plan. Phys., U of Cal (Riverside) CA 92521, May 1977.

LeSchack, L.A., Lewis, J.E., Chang, D.C., 1977, Rapid Reconnaissance of Geothermal Prospects Using Shallow Temperature Surveys. Development and Resources Transportation Co. (now LeSchack Associates, Ltd.) Silver Spring, Md. 20902, Semi-Annual Tech. Rept. under Contract EG-77-C-01-4021 for the U.S. Dept. of Energy.

LeSchack, L.A., Lewis, J.E., Chang, D.C., Lewellen, R.I. and O'Hara, N.W., 1979, Rapid Rkconnaissance of Geothermal Prospects Using Shallow Temperature Surveys, Second Tech. Rept. by LeSchack Associates Ltd., Silver Spring, Md 20902 under U.S. Dept. of Energy Contract EG-77-C-01-4021 and Office of Naval Research Contract N00014-78-C-0535.

Lettau, H.H., 1969, Note on Aerodynamic Roughness--Parameter Estimation on the Basis of Roughness--Element Description, J. Applied Meteorology, V8, No 5, pp 828-832.

Montieth, J.L., 1973: Principle of Environmental Physics, Edward Arnold, London.

Oke, T.R., 1978: Boundary Layer Climates, Methuen Co., London.

Outcalt, Sam I., 1972, The Development and Application of a Simple Digital Surface Climate Simulator, Jour. of Applied Meteorology, V11, No 4, pp 629-636.

Paulson, C.A., 1970: The mathematical representative of wind speed and temperature in the unstable atmospheric surface layer. J. Appl. Meteor, 9, 857-861.

Pease, R. *et al*, 1976, Urban terrain climatology and remote sensing, Annals of Assoc. Amer. Geog., 66, 557-569.

Sellers, William D., 1965: Physical Climatology, University of Chicago Press, Chicago.

APPENDIX 1

by Kevin McNamee

Evaluating the Lee FINITEG Program

The area to be studied by FINITEG is a two-dimensional region (horizontal distance is the ordinate, depth is the abscissa) consisting of four sides, three of which are straight lines, while the top side is a topographic representation or profile of the area. When entering the data, the topographic coordinates of the area to be studied must be specified. The defined study area is then divided into quadrilaterals formed by rows and columns. The width of the quadrilaterals is decided by the user. The greater the number of rows and columns, the greater the resolution of the model. The program attaches coordinates to the nodal points of this quadrilateral framework. Right-handed rectangular coordinates are used and the origin is set at the lower left-hand corner. The field data (i.e., thermal conductivity, surface temperature, etc.) are then assigned to this region by the user. Basically the same procedure is followed for the anomalous regions except that they are not broken into discrete elements. Their global coordinates within the defined study area as well as their extreme coordinates are entered into the program. The data used for the study at Coso follow:

The area chosen for this heat flow study was an east-west transect through Cactus Peak extending from, east to west, stations 62, 61, 63 and 64. The transect is 7.2 kilometers long and the base of the region is at 0.7 kilometers above sea level. Three anomalous soil regions were considered in this area. They are on either side of Cactus Peak. Their global coordinates are listed below along with their physical description.

The data input consists of a number of input cards. The first card is the title. On the second card the input is as follows: (1) NX is the number of columns (=36). Each column has a horizontal width of 0.2 kilometers. The number of columns and rows is chosen by the user. (2) NY is the number of rows (=22). The spacing of the rows is based on a geometrical progression--the closer to the surface, the smaller the spacing. This provides for finer resolution in the upper part of the subsurface. FINITEG allows the user to choose the row spacing by merely changing program cards. For our purposes, geometrical spacing was used for better near-surface resolution. Since the program input is in km, however, the resolution is poor in the upper 9 m. (3) NDT is the number of time increments (=1); this is the steady state condition. (4) NREG is the number of anomalous regions (=3). (5) NBC is the type of boundary condition chosen (=2). This specific boundary condition occurs when there are surface temperatures

given at the top of the boundary area and a known heat flux at the bottom of the boundary area. (6) JFLUX is the Jth row at which the calculations for nodal temperature and net flux are calculated (=NY=22). In this case, the calculations proceed to the top of the study area. (7) MOVE is the topographic surface movement (=0).

On the third input card, the physical data of the area broken into discrete elements are included. The first variable is DT, the time increment for transient temperature solutions. For the steady state condition, DT=0. The units are in millions of years. The physical data, derived from Combs (1976) are as follows: (1) AK is the regional thermal conductivity, = 2.762 W/mK^{O}, (2) DIFU is the diffusivity, = 1.27 x 10^{-6} m^2/sec, (3) AQ is the regional heat production, and for this transect it was assumed that there were no heat sinks or sources, therefore, AQ is zero, (4) ALAPSE is the lapse rate and is $31.5^{O}C/m$, and (5) QIN is the input heat flux to the bottom of the model area and is 87.99 mW/m^2*.

On the fourth card the topographic data are entered; TOPO (I, 1) is horizontal distance, and TOPO (I,2) is height. In the case of Coso, there are 37 topographic points entered. The 7.2 km east-west transect was divided evenly into 36 columns, each 0.2 km long. To find TOPO (I,2), a topographic profile was drawn from a topographic map of the Coso area. The TOPO (I,1) coordinates were plotted on the topographic profile and the height was read to give TOPO (I,2). These data were then converted to kilometers. The TOPO (I,2) data were calculated from a base value of 0.7 km ASL. The base was given the value TOPO (I,2) = 0 and the height of the topographic point was calculated accordingly.

For each anomalous soil region, a number of inputs are required. On the topographic profile, the anomalous soil regions are numbered from left to right so that the data input for each anomalous region must follow in sequential order. (1) NPT is the number of vertices of a polygon surrounding the nth anomalous region, and (2) COND is the conductivity. For anomalous regions 1 and 3, COND is 0.2078 $W/m \cdot K^{O}$ and for anomalous region, 2, COND is 0.1837 $W/m \cdot K^{O}$. (3) CAPA is the thermal diffusivity of the anomalous region. For regions 1 and 3 CAPA is 0.158 x 10^{-6} m^2/sec and for region 2 CAPA is 0.140 x $10^{-6} m^2/sec$. (4) HEAT is the heat generation and is zero. (5) EXTREMA are the topographic points needed to define the extreme coordinates X_{left}, X_{right}, Y_{lower}, and Y_{upper} of each anomalous region.

The coordinates of each vertex must now be defined for

*We have used SI units here to be consistent with Lee's model, rather than changing them to the CGS units used in the body of the report.

each anomalous region. If NPT is 10, there must be 10 global coordinates, defined as REG (K, 1) and REG (K, 2)(horizontal and vertical component). The coordinates are read counter-clockwise starting from the lower left of each anomalous soil quadrilateral (see Figure 4 of the text).

The last input is the boundary temperature at the top of the surface. The original program called for the surface temperatures to be set at 0°C, but this was modified for our purposes so that we could enter our 2-m temperatures. There is a 2-m temperature to correspond with each topographic surface coordinate. In effect, the surface of this model is at a 2-m depth. We felt this justifiable due to the lack of resolution in the top 5 m.

The surface temperature is a uniform 21.3° Celcius. This was derived by consulting a SYMMAP*-produced 1° C-interval temperature map for corrected mean annual temperatures at Coso. In the area of Cactus Peak, the temperatures were found to be a uniform 21.3°C at the 2 m depth.

The output of program FINITEG are 851 temperature nodes (37 horizontal nodes x 23 vertical nodes), and these are mapped onto the study area. Since the rows are geometrically spaced and the total length of each column is different due to the topography, the width of each row from column to column will differ. The width of each row is calculated by substituting the total length of each column and the number of rows into the geometric spacing equation:

$$(J-1)\ |2(N_y + 1) - J|\ TOPO(I, 2)/N_y(N_y + 1)$$

where J is the row number. N_y the total number of rows to be calculated, and TOPO(I, 2) the total length of the column. From this, we can plot the position of each nodal point, and its associated temperature and finally, isotherms.

*See Appendix 2

Reference

Combs, J., 1976, The Coso Geothermal Project, Tech. Rept. No. 3, Dec. 1976, Heat Flow Determinations in the Coso Geothermal Area, California, Battelle Northwest Laboratories, Richland, Wash. 99352 and Center for Energy Studies, Univ. of Texas at Dallas, Richardson, Tx 75080 under Contract E(45-1)-1830, ERDA.

APPENDIX 2

Map Contouring by SYMMAP

We tried to avoid bias when contouring our data for presentation, especially when comparing our anomalies with those generated by other researchers. Our data were contoured by the SYMAP computer program (version 5.20) designed by the Laboratory for Computer Graphics and Spatial Analysis, Graduate School of Design, Harvard University, Cambridge, Massachusetts, 02138. The program takes the maximum and minimum points in a data set and obtains their difference. The difference value is divided by five, forming five equi-dimensional cells. The numerical boundary between the lowest and next lowest cell becomes the value of the lowest contour. The next highest contour is the boundary between the second lowest and the middle cell, for a total of four contour lines. Contour values and intervals are derived when the data set is specified. Different typographic characters are used to "fill in" the space between contours. In each field of characters, numbers from 1 to 5 correspond to geographic locations of the data points being contoured. A figure "1" represents the location of a given point whose range falls within the confines of the lowest cell. A figure "5" represents the location of a data point in the highest cell.

UNCLASSIFIED

Security Classification

AD-A083 953

DOCUMENT CONTROL DATA - R & D

(Security classification of title, body of abstract and indexing annotation must be entered when the overall report is classified)

1. ORIGINATING ACTIVITY *(Corporate author)*

LeSchack Associates, Ltd.
1111 University Blvd. West
Silver Spring, Maryland 20902

2a. REPORT SECURITY CLASSIFICATION

UNCLASSIFIED

2b. GROUP

3. REPORT TITLE

RAPID RECONNAISSANCE OF GEOTHERMAL PROSPECTS USING SHALLOW TEMPERATURE SURVEYS

4. DESCRIPTIVE NOTES *(Type of report and inclusive dates)*

Third report for DOE, Final Report for ONR

5. AUTHOR(S) *(First name, middle initial, last name)*

Leonard A. LeSchack, John E. Lewis, David C. Chang

6. REPORT DATE

March 1980

7a. TOTAL NO. OF PAGES

32

7b. NO. OF REFS

14

8a. CONTRACT OR GRANT NO.

N00014-78-C-0555 (ONR)
EG-77-C-01-4021 (DOE)

NR-081-317 (ONR)

9a. ORIGINATOR'S REPORT NUMBER(S)

DOE/ONR 3

9b. OTHER REPORT NO(S) *(Any other numbers that may be assigned this report)*

N/A

10. DISTRIBUTION STATEMENT

Distribution of this document is unlimited

11. SUPPLEMENTARY NOTES

Work discussed in this report was supported equally by DOE and ONR

12. SPONSORING MILITARY ACTIVITY

Office of Naval Research
800 N. Quincy Street
Arlington, Virginia 22217

13. ABSTRACT

In this final report, an Annual Wave Correction Model is constructed. The model makes rapid reconnaissance of geothermal prospects using shallow temperature surveys a reality.

The model is tested using data previously obtained at the Coso KGRA. Inputs are surface meteorological data gathered during a 15 month period, soil thermal diffusivity data derived from previous studies in this series, and surface roughness and albedo measured at the site. Computations are made to determine the normal, i.e., non-anomalous temperatures at 2-m depth, for the period 22-24 September 1977, for each of the 102 stations at Coso. The observed 2-m temperatures recorded at these stations during this period and corrected for elevation are compared to the normal temperatures, and a residual anomaly map has been drawn. The map compares favorably to the mean annual temperature map for the same area.

We conclude that a 2-m temperature survey may be conducted at any time and appropriately corrected with the Annual Temperature Correction Model and easily obtained ancillary data. Our model produces a residual map with an accuracy of $\pm$ 1.9°C, adequate for anomalies of the magnitude found at Coso.

We studied the effect of topography on sub-surface isotherms at Coso KGRA using a model (FINITEG) developed by Lee. The model predicted sub-surface temperatures to a depth of 0.75 km in the area of Cactus Peak. The model takes into account 100 m of topographical change and the effects of three anomalous regions near the surface, representing the soil in which the measurements were made. Within the resolution of

DD FORM 1 NOV 68 1473 REPLACES DD FORM 1473, 1 JAN 64, WHICH IS OBSOLETE FOR ARMY USE.

UNCLASSIFIED 394 287

Security Classification

14 KEY WORDS	LINK A		LINK B		LINK C	
	ROLE	WT	ROLE	WT	ROLE	WT
Geothermal reconnaissance surveys SHALLO-TEMP™ surveys (a shallow temperature exploration technique) Annual wave model Coso KGRA, Naval Weapons Center, China Lake, California						

ABSTRACT continued

the model, the isotherms conform to the topography; the contour interval is essentially unvarying as it approaches the surface, even though the isotherms pass through thin soil layers of different thermal conductivity.

We conclude that in geological settings in the Basin and Range Province, where there is some topographic relief layer overlying a more conductive bedrock, there are no significant distortions to a 2-m temperature contour map. We can emplace our 2-m survey holes with relatively little concern for topography or modest variations in soil conditions.